

DYNAMIC STRAIN AGING BEHAVIOR OF INCONEL 600 ALLOY

Soon H. Hong, Hee Y. Kim, Jin S. Jang* and Il H. Kuk*

Dept. of Materials Science and Engineering,
Korea Advanced Institute of Science and Technology
373-1 Kusung-dong, Yuseong-gu, Taejeon, 305-701, Korea

* Korea Atomic Energy Research Institute,
P.O. Box 105, Yuseong, Taejeon, 305-600, Korea

Abstract

The dynamic strain aging behavior during tensile tests of Inconel 600 alloy has been investigated in the temperature range of 25-800°C over the strain rate range of 10^{-5} - 10^{-3} s⁻¹. The serrations in flow curves were observed in the temperature range of 150-600°C. Four different types of serrations, identified as A1, A2, B and C serrations, were observed depending on the temperature, strain rate and strain. A1 type serration, a periodic rise and drop of stress with small amplitude, was observed in the temperature range of 150-245°C. A2 type serration, a rise of stress followed by a drop of stress, was observed at a higher temperature range of 245-400°C. B type serration, a successive oscillation of stress, was observed in the temperature range of 245-500°C. C type serration, characterized as abrupt irregular stress drops, was observed in the temperature range of 600-700°C. The activation energies for the serrated flow were calculated as 105, 81 and 150kJ/mol for A1, A2 and B type serration, respectively, from the analysis of the critical strains for onset of serrations. The rate controlling mechanism for dynamic strain aging is suggested as the migration of substitutional atoms for A1 type serration, carbon diffusion through dislocation core for A2 type serration and carbon diffusion through lattice for B type serration.

Introduction

Inconel 600 alloy is a Ni-base austenitic solid solution alloy which has been used as steam generator tubes in pressurized water reactors of nuclear power plant due to its good mechanical strength, thermal conductivity and corrosion resistance. There have been extensive studies on the stress corrosion cracking behavior of Inconel 600 alloy because the main failure mode of steam generator tube is due to stress corrosion. The susceptibility of Inconel 600 alloy to stress corrosion cracking depends on composition, microstructure, environment and stress state. Recently, it is reported that stress corrosion cracking is related to the microdeformation[1, 2] and creep[3]. Therefore, it is important to understand the deformation behavior of Inconel 600 alloy.

Several researchers[4-6] have observed the serrated plastic flow and high work hardening rates with negative strain rate sensitivity in Inconel 600 alloy, however the controlling mechanism for the serration is not clearly understood yet. It is generally accepted that the serration in stress-strain curve is attributed to the dynamic strain aging of solute atoms. Hayes and Hayes[5] reported that the activation energy for the onset of serration is 54kJ/mol in Inconel

600 and suggested that dynamic strain aging phenomena are primarily caused by the diffusion of carbon rather than the substitutional atoms (primarily Fe and Cr) on the basis of the similar activation energy for onset of serration in Ni-C alloys. However, the temperature regime showing the serration in Inconel 600 is much higher than that showing the serration in Ni-C alloys[7]. Kocks[6] reported that the serration behavior of low carbon content below 0.05at.% in Inconel 600 was identical to that of commercial Inconel 600 alloy. These results are contradictory to the results of Hayes and Hayes[5].

In this paper, the controlling mechanisms of serrated flow in Inconel 600 alloy were analysed. The serrated flow in Inconel 600 alloy during tensile tests has been investigated at temperatures of 25-800°C with strain rates ranging 10^{-5} - 10^{-3} s⁻¹. The stress-strain curves and types of serration were analysed. The activation energies of each type of serration were evaluated by the critical strain method and the controlling mechanisms for each type of serration will be discussed.

Experimental Procedures

Inconel 600 alloy was melted in a vacuum induction melting furnace and cast into ingots of 1180kg by Sammi Special Steel Co., LTD. The chemical composition of melted alloy is given in Table I. The cast ingots were forged at 1250°C and were hot extruded into tubes at 1200°C. The extruded tubes were cold worked into 1.06mm thick tubes by the pilgering with 96% reduction. The tubes were annealed at 1030°C for 20 minutes. The thermal treatment of annealed tubes was conducted at 700°C for 10 hours in Ar atmosphere to precipitate the carbides at grain boundaries. The average grain size was measured as 38µm after thermal treatment. The tensile specimens were machined from thermal treated Inconel 600 tubes and were tested in the temperature range of 25-800°C over the strain rate range of 10^{-5} - 10^{-3} s⁻¹. The serration behaviors depending on temperature, strain rate and strain were analysed from the stress-strain curves. The critical strains for onset of serration were measured from the stress-strain curves and the activation energies for onset of serration were evaluated by the critical strain method.

Table I Chemical composition of Inconel 600

Element	Ni	Cr	Fe	Ti	Si	Mn	C	N
wt. %	76.88	15.55	6.98	0.28	0.16	0.23	0.02	0.0004

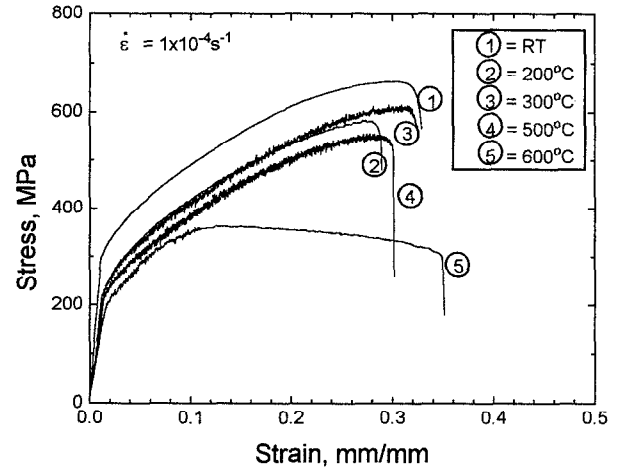
Results and Discussion

The observed stress-strain curves of Inconel 600 alloy with varying temperature and strain rate are shown in Figure 1. The serrated stress-strain curves were observed at temperatures between 300°C and 600°C under initial strain rate of 10^{-4}s^{-1} as shown in Figure 1(a). It is obvious that the work hardening rate is high within the temperature regime showing serrated stress-strain curves. The inverse strain rate dependence of flow stress is exhibited at temperature showing the serration as shown in Figure 1(b). Typical segments of the stress-strain curves during tensile tests of Inconel 600 are shown in Figure 2. Four different types of serration were reported and are classified as type A, type B, type C and type E, depending on the strain rate, temperature and strain[8]. Type A serration is characterized as periodic serration which is an abrupt rise of stress followed by a drop of stress in the stress-strain curve. Type B serration is characterized as successive oscillations of stress in the stress-strain curve, while type C serration is characterized as abrupt irregular stress drop. Type E serration is characterized as a random irregular drop of stress. Smooth flow curves without any serration were observed at temperatures below 150°C. Type A serration characterized as a periodic rise and drop of stress with small amplitude was observed at a lower temperature range of 150-245°C. Different type A serration characterized as a rise of stress followed by a drop of stress was observed at a higher temperature range of 245-400°C. Two different type A serrations were observed in the temperature range of 150-245°C and 245-400°C, and were designated as A1 type serration and A2 type serration, respectively. Type A serration changed into type E after certain amount of strain. Type B serration was observed at temperatures above 245°C and the amplitude of stress drop increased with increasing temperature up to 600°C. It is observed that type B serration was superimposed on type A serration at a temperature range of 245-400°C. Type C serration was observed at higher temperatures above 600°C. The temperature regime showing the different types of serrations varied systematically with strain rate. The regimes of various types of serration depend on the strain rate and temperature as shown in Figure 3.

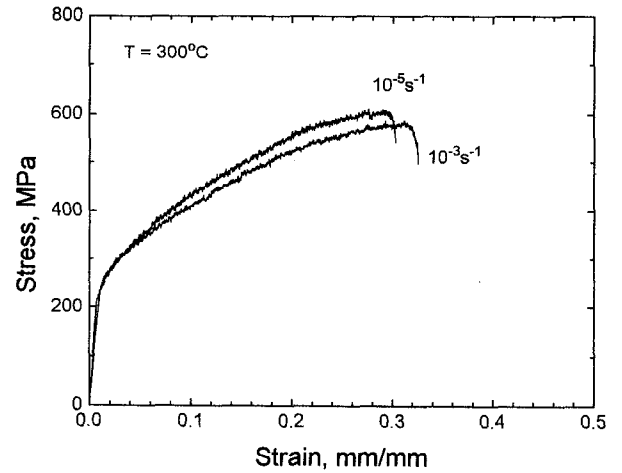
It is well established that a critical amount of plastic strain is needed to initiate the serration on the stress-strain curves. The previous results[9] on the serrated flow suggest that the dependence of critical strain for onset of serration (ϵ_c) on strain rate and temperature is generally expressed as following Eq. (1),

$$\epsilon_c^{m+\beta} = K\dot{\epsilon}\exp(Q/RT) \quad (1)$$

where Q is the activation energy for onset of serration, m and β are the strain exponents related with the vacancy concentration C_v and mobile dislocation density ρ_m , i.e. $C_v \propto \epsilon^m$, $\rho_m \propto \epsilon^\beta$, and K is constant. The activation energies, Q , for onset of each type of serration were measured by three different methods. First, Q was evaluated from the slope of a plot $\log \epsilon_c$ vs $1/T$ at a constant strain rate in Eq. (1). It can be obtained the exponent $m + \beta$ from the slope of a plot of $\log \dot{\epsilon}$ vs $\log \epsilon_c$ at a constant temperature. Second, Q is evaluated from the plot of $\log \dot{\epsilon}$ vs $\log \epsilon_c$. The strain rates corresponding to fixed value of critical strains were obtained from Figure 4. The replot of the obtained strain rates with varying temperature yield straight lines and Q is obtained from the slope of the lines. Third, Q is evaluated using McCormick's strain aging model[10] expressed as Eq. (2),



(a)



(b)

Figure 1: The observed stress-strain curves of Inconel 600 alloy. (a) The stress-strain curves with varying the temperature at the initial strain rate of 10^{-4}s^{-1} . (b) The stress-strain curves with varying the initial strain rate at constant temperature of 300°C.

$$\frac{\epsilon_c^{m+\beta}}{T} = \left(\frac{C_1}{\phi C_0} \right)^{3/2} \frac{\dot{\epsilon} k b \exp(Q/kT)}{L N U_m D_0} \quad (2)$$

where C_0 is initial concentration of solute in the alloy, C_1 is local concentration of the solute at dislocations, L is obstacle spacing, U_m is maximum solute-dislocation interaction energy, D_0 is frequency factor, b is Burgers vector and N and ϕ are constants. Q is obtained from the slope of a plot of $\log(\epsilon_c^{m+\beta}/T)$ vs $1/T$ plot[11].

The critical strain for onset of serration, ϵ_c , was measured from the stress-strain curves. The variation of ϵ_c with varying strain rate and temperature for A1, A2 and C type serrations are shown in Figure 4. The values of $m+\beta$ were calculated as 2.15 for A1 type, 1.02 for A2 type and 1.04 for B type serration. The activation energies for onset of each type serration were calculated from the slopes a plot of $\log \epsilon_c$ vs $1/T$ as shown in Figure 5. The activation

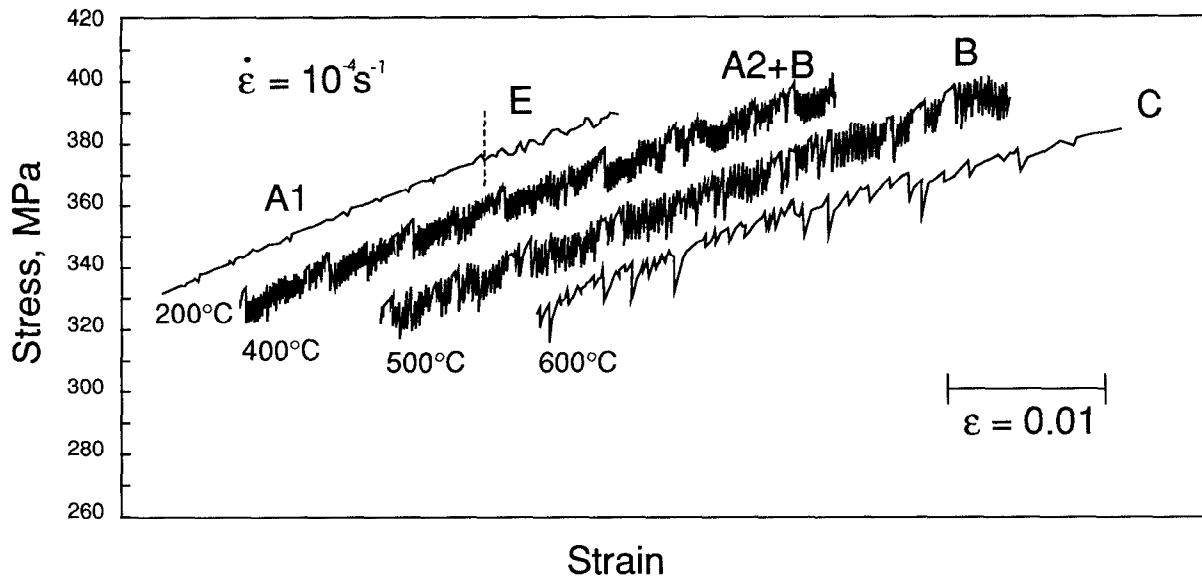


Figure 2: Various types of serrated flow observed in stress-strain curves of Inconel 600 alloy during tensile tests with strain rate of 10^{-4} s^{-1} at various temperature.

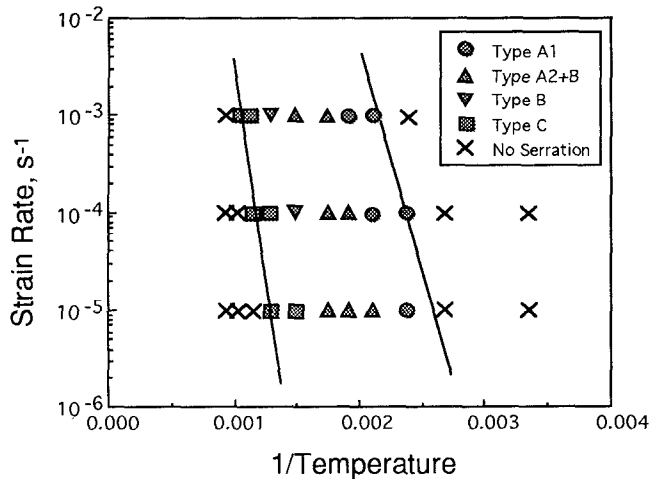


Figure 3: The observed range of temperature showing the various types of serrations in stress-strain curves of Inconel 600 alloy at different strain rates.

energies were also calculated by other methods described above. It is calculated from a plot of $\log \dot{\epsilon}$ vs $1/T$ using intercept method and from a plot of $\log(\dot{\epsilon}_c^{m+\beta}/T)$ vs $1/T$ using Cottrell-Bilby equation as shown in Figure 6 and Figure 7. The calculated values of $m+\beta$ and Q for each type serration are listed in Table II.

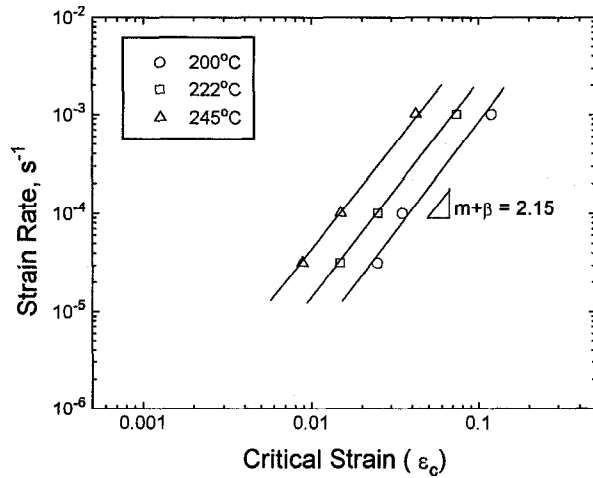
It is generally known that the values of $m+\beta$ ranged 0.5-1 for dynamic strain aging is due to the interstitial solute, whereas the values of $m+\beta$ ranged 2-3 for dynamic strain aging is due to the substitutional solute in solid solution alloys[9]. The $m+\beta$ values were measured as 0.63 in Ni-C[7] and 0.72 in Fe-C[12], while 2.4 in Au-Cu[13], 2-3 in Cu-Zn[14] and 3.33 in Al-Mg-Zn[15]. Comparing the calculated $m+\beta$ values in Table II with those

Table II The activation energies calculated by different methods for Inconel 600

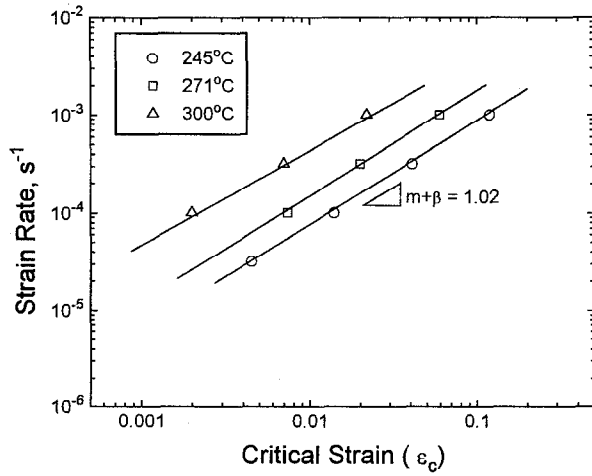
	Activation Energy for Onset of Serration, kJ/mol		
	A1 type serration	A2 type serration	B type serration
From $\log \dot{\epsilon}_c$ vs $1/T$ plot	95	84	144
From $\log \dot{\epsilon}$ vs $1/T$ plot	127	72	163
From $\log(\dot{\epsilon}_c^{m+\beta}/T)$ vs $1/T$ plot	93	87	144
Average Q	105	81	150
Average $m+\beta$	2.15	1.02	1.04

reported in solid solution alloys, it is suggested that the onset of A1 type serration was controlled by substitutional element in Inconel 600 alloy, while the onset of A2 type serration and B type serration were controlled by interstitial element in Inconel 600 alloy. The activation energy measured as 105kJ/mol for the onset of A1 type serration is close to the activation energy for vacancy migration of 106kJ/mol in Ni. The activation energy for vacancy migration in Ni is calculated from the difference of the activation energy for self diffusion of 280kJ/mol[16] and the activation for vacancy formation of 174kJ/mol[17]. Therefore, it is suggested that A1 type serration is controlled by the migration of the substitutional solute atoms in Inconel 600 alloy. The major substitutional elements in Inconel 600 are Cr, Fe, Ti and Mn as shown in Table I. Ti is considered as the most possible element for dynamic strain aging related with A1 type serration in temperature regime of 150-245°C, because the difference in atomic size of solute and solvent atom of Ti is the largest.

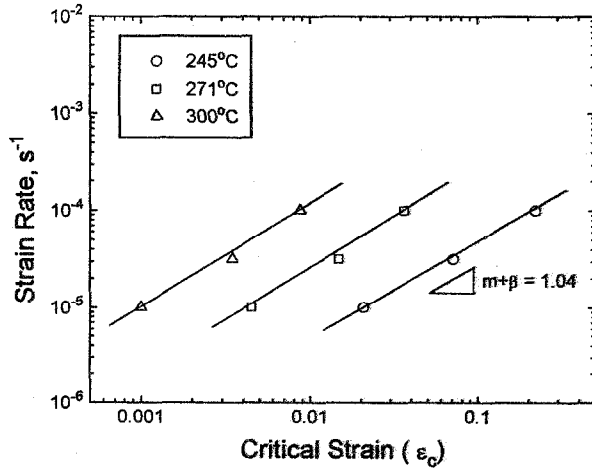
The activation energy for onset of A2 type serration measured as



(a)

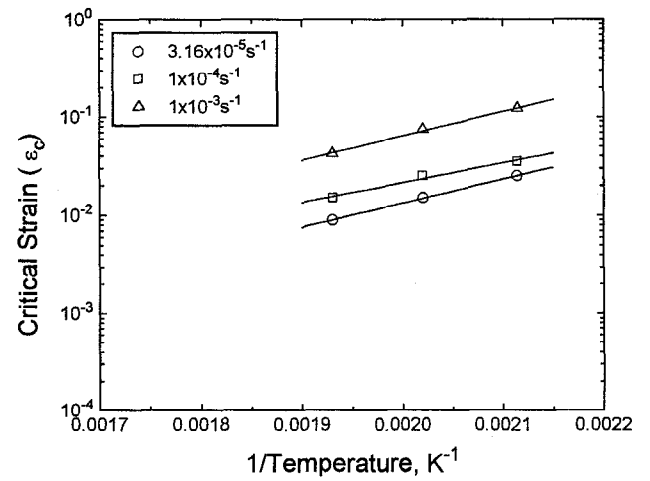


(b)

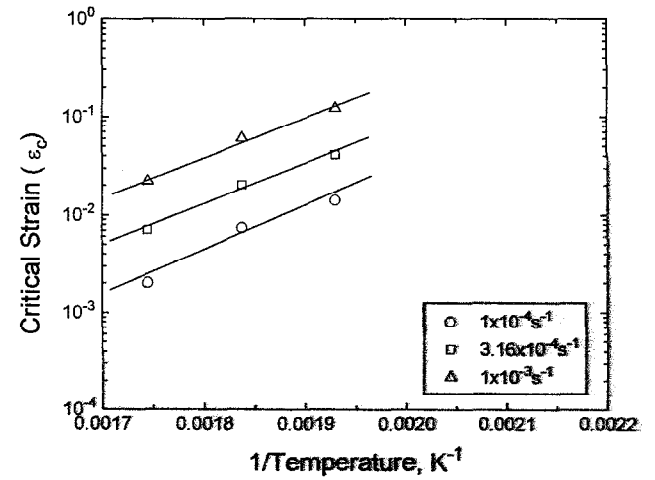


(c)

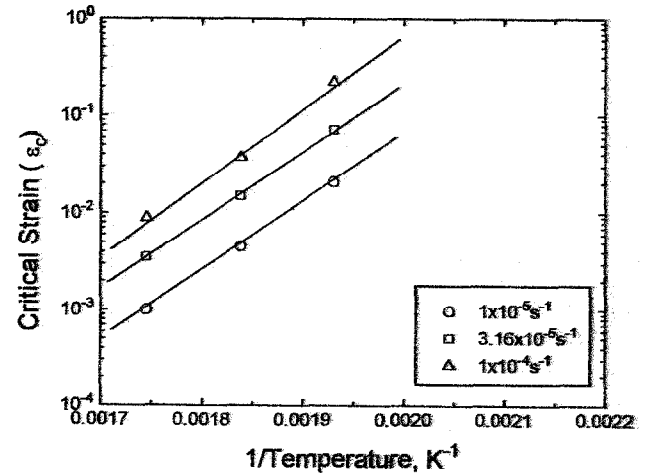
Figure 4: The variation of critical strain for onset of serration in stress-strain curve of Inconel 600 alloy with varying strain rate. (a) A1 type serration, (b) A2 type serration, (c) B type serration.



(a)



(b)



(c)

Figure 5: The variation of critical strain for onset of serration in stress-strain curve of Inconel 600 alloy with varying temperature. (a) A1 type serration, (b) A2 type serration, (c) B type serration.

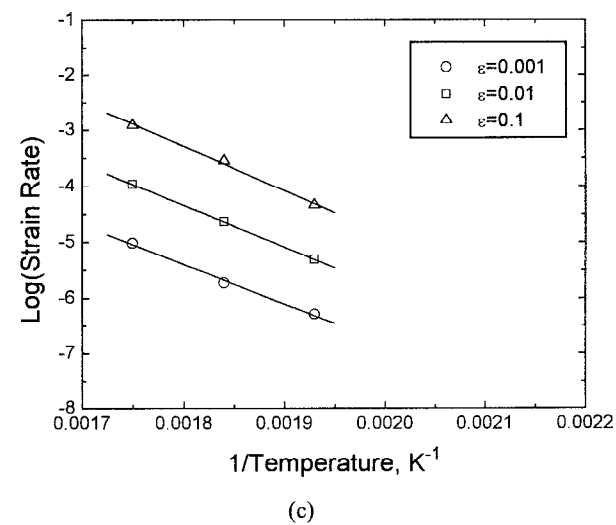
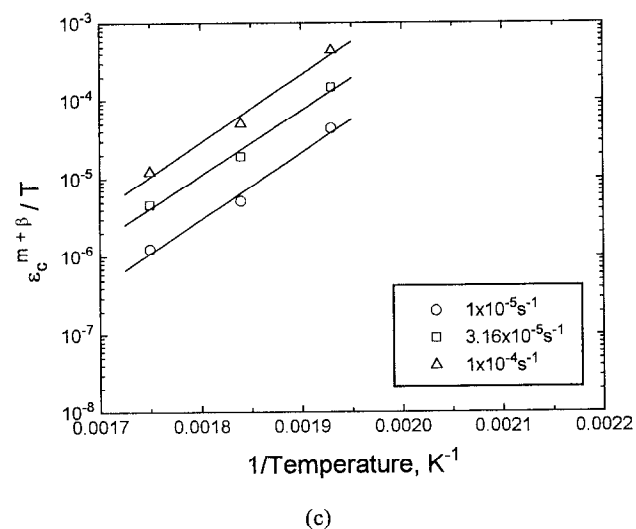
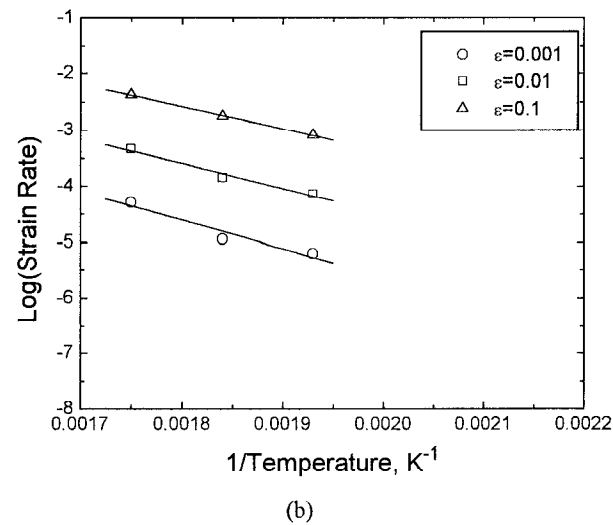
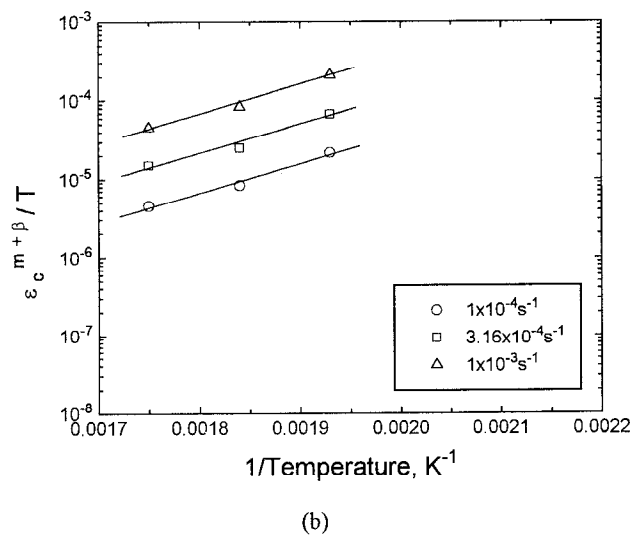
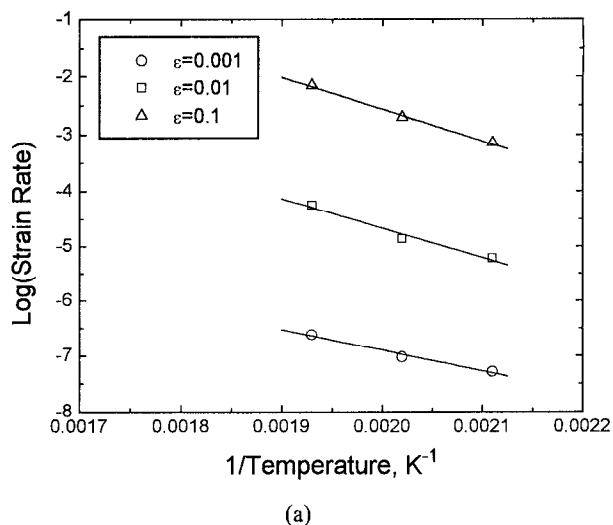
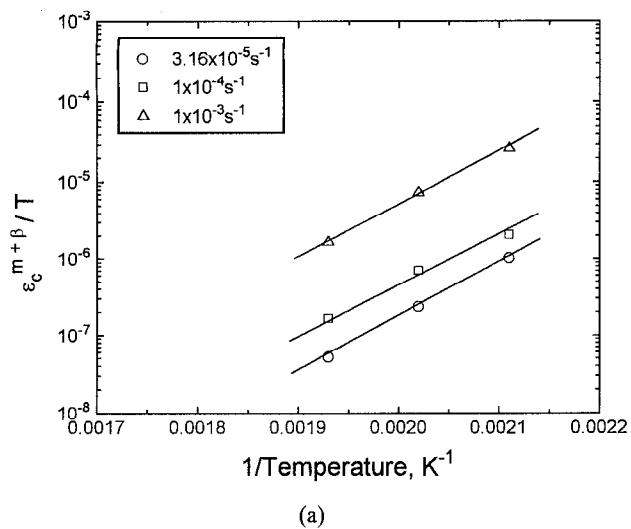


Figure 6: The variation of $\log(\epsilon_c^{m+\beta}/T)$ measured from the stress-strain curve of Inconel 600 alloy with varying temperature. (a) A1 type serration, (b) A2 type serration, (c) B type serration.

Figure 7: The variation of the strain rate corresponding to fixed value of critical strains in Figure 4 with varying temperature. (a) A1 type serration, (b) A2 type serration, (c) B type serration.

81kJ/mol. The A2 type serration observed in this study is comparable to the serration in Inconel 600 observed by Hayes and Hayes[5] and in Ni-C observed by Nakada and Keh[6]. Hayes and Hayes[5] reported the $m+\beta$ is 0.74 and Q is 54kJ/mol in Inconel 600 alloy in the temperature range of 316-538°C, while Nakada and Keh[7] reported that that $m+\beta$ is 0.63 and Q is 63kJ/mol in pure Ni-C alloys in the temperature range of -50-300°C. It is suggested that carbon is the rate controlling element because it is the major interstitial element in Inconel 600. It is reported that the activation energy for lattice diffusion of C in Ni is 139kJ/mol[18]. Since the ratio of activation energy for dislocation pipe diffusion to that for lattice diffusion, $Q_{\text{disl}}/Q_{\text{lattice}}$, is generally known as 0.65 in fcc metals[19]. The Q_{disl} is calculated to be 90kJ/mol and is quite similar to the measured activation energy for onset of A2 type serration. Also, the measured activation energy for onset of A2 type serration is similar to the activation energy for onset of serration in Ni-C reported by Nakada and Keh[7]. Therefore, the rate controlling mechanism for onset of A2 type serration is suggested as the carbon diffusion through dislocation core.

The activation energy for onset of B type serration measured as 150kJ/mol, which is similar to the activation energy of 139kJ/mol for carbon diffusion in Ni[18]. The controlling mechanism of B type serration is suggested as the carbon diffusion in Inconel 600. Kocks et al.[6] reported that the serration behavior of Inconel 600 with low carbon less than 0.05at.% was identical to that of commercial Inconel 600. They suggested that the dynamic strain aging in Inconel 600 is more likely controlled by solute atoms rather than carbon. However, the low values of $m+\beta$ indicate that the substitutional atom - carbon compounds could retard the diffusion rate of carbon and are responsible element for A2 and B type serrations, as suggested in austenitic stainless steels[20, 21]. The possible substitutional elements are Cr and Ti due to their strong tendency to form carbides. The amount of carbon in Inconel 600 alloy needed to pin the dislocation for onset of serration could be very low when the substitutional atom - carbon compounds interact with dislocations.

Conclusions

The serrations in stress strain curves due to dynamic strain aging were observed in the temperature range of 150-600°C with a strain rate of 10^{-5} - 10^{-3} s⁻¹ in Inconel 600 alloy. Four different types of serration, A1, A2, B and C type serration, were observed depending on the temperature, strain rate and strain. A1 type serration, a periodic rise and drop of stress with small amplitude, was observed in the temperature range of 150-245°C. A2 type serration, a rise of stress followed by a drop of stress, was observed at a higher temperature range of 245-400°C. B type serration, successive oscillations of stress, observed in the temperature range of 245-500°C. C type serration, characterized as abrupt irregular stress drops, was observed at a temperature of 600°C. The higher work hardening rate and negative strain rate sensitivity were observed within the temperature regime showing serrated stress-strain curves. Based on the analysis of $m+\beta$ and Q , the rate controlling mechanisms are suggested as the migration of substitutional atoms for A1 type serration, carbon diffusion through dislocation core for A2 type serration and carbon diffusion through lattice for B type serration. The diffusion of the substitutional atom - carbon compounds could be the rate controlling mechanism for A2 and B type serration.

References

1. S. M. Bruemmer and C. H. Henager, Jr., "High Voltage Electron Microscopy Observations of Microdeformation in Alloy 600 Tubing," *Scr. Metall.*, 20 (1986), 909-914.
2. S. M. Bruemmer, "Microstructure and Microdeformation Effects on IGSCC of Alloy 600 Steam Generator Tubing," *Corrosion*, 44 (1988), 782-788.
3. G. A. Was, J. K. Sung and T. M. Angelu, "Effect of Grain Boundary Chemistry on the Intergranular Cracking Behavior of Ni-16Cr-9Fe in High Temperature Water," *Metall. Trans.*, 23A (1992), 3343.
4. R. A. Mulford and V. F. Kocks, "New Observation on the Mechanisms of Dynamic Strain Aging and of Jerky Flow," *Acta Metall.*, 27 (1979), 1125-1134.
5. R. W. Hayes and W. C. Hayes, "On the Mechanism of Delayed Discontinuous Plastic Flow in an Age-Hardened Nickel Alloy," *Acta Metall.*, 30 (1982), 1295-1301.
6. U. F. Kocks, R. E. Cook and R. A. Mulford, "Strain Aging and Strain Hardening in Ni-C Alloys," *Acta Metall.*, 33 (1985), 623-638.
7. Y. Nakada and A. S. Keh, "Serrated Flow in Ni-C Alloys," *Acta Metall.*, 18 (1970), 437-443.
8. B. J. Brindley and P. J. Worthington, "Yield Point Phenomena in Substitutional Alloys," *Metall. Rev.*, 145 (1970), 101-114.
9. A. Van den Beukel, "On the Mechanism of Serrated Yielding and Dynamic Strain Aging," *Acta Metall.*, 28 (1980), 965-969.
10. P. G. McCormick, "A Model for the Portevin-Le Chatelier Effect in Substitutional Alloys," *Acta Metall.*, 20 (1972), 351-354.
11. I. S. Kim and M. C. Chaturvedi, "Serrated Flow in Inconel 625," *Trans. JIM*, 28 (1987), 205.
12. P. G. McCormick, "The Portevin-Le Chatelier Effect in a Pressurized Low Carbon Steel," *Acta Metall.*, 21 (1973), 873-878.
13. A. Wijler, M. M. A. Vrijhoef and A. Van den Beukel, "The Onset of Serrated Yielding in Au(Cu) Alloys," *Acta Metall.*, 22 (1974), 13-19.
14. D. Munz and E. Macherauch, "Dynamische Reckalterung von α -Messing," *Z. Metallk.*, 57 (1966), 552-559.
15. K. Mukherjee, C. D'Antonio, R. Maciag and G. Fisher, "Impurity-Dislocation and Reported Yielding in a Commercial Al Alloy," *J. Appl. Phys.*, 39 (1968), 5434.
16. A. M. Brown and M. F. Ashby, "Correlations for Diffusion Constants," *Acta Metall.*, 28 (1980), 1085.
17. J. Friedel, *Dislocations*, (Oxford: Pergamon, 1964), 102.

18. C. J. Smithells, *Metals Reference Book*, Vol. 2, 4th ed. (Plenum Press, 1967), 649.
19. D. D. Pruthi, M. S. Anand and R. P. Agarwala, "Diffusion of Chromium Inconel-600," J. Nucl. Mater., 64 (1977), 206.
20. L. H. De Almeida, I. Le May and S. N. Monteiro, Strength of Metals and Alloys, (Pergamon Press, 1986), 337.
21. S. Venkadesan, C. Phaniraj, P. V. Sivaprasad and P. Rodriguez, "Activation Energy for Serrated Flow in a 15Cr-15Ni Ti-Modified Austenitic Stainless Steel," Acta Metall. Mater., 40 (1992), 569-580.